Published in final edited form as:

J Invest Dermatol. 2016 July ; 136(7): 1449–1459. doi:10.1016/j.jid.2016.02.814.

The Parathyroid Hormone Second Receptor PTH2R and its Ligand Tuberoinfundibular Peptide of 39 Residues TIP39 Regulate Intracellular Calcium and Influence Keratinocyte Differentiation

Emi Sato[1], **Jun Muto**[2], **Ling-Juan Zhang**[1], **Christopher A. Adase**[1], **James A. Sanford**[1], **Toshiya Takahashi**[1], **Teruaki Nakatsuji**[1], **Ted B. Usdin**[3], and **Richard L. Gallo**[1]

[1]Department of Dermatology, University of California San Diego, La Jolla, California, USA

[2]Department of Dermatology, Aichi Medical University, Nagakute, Aichi, Japan

[3]Section on Fundamental Neuroscience, NIMH National Institute of Mental Health, Bethesda, Maryland, USA

Abstract

Genes related to the parathyroid hormone (PTH) influence cutaneous immune defense and development, but the full functions of the PTH family in cutaneous biology remain incompletely understood. In this study, we examined the expression and potential functions of the PTH second receptor (PTH2R) and its ligand, the tuberoinfundibular peptide of 39 residues (TIP39), in the skin. TIP39 and PTH2R mRNA and protein were detectable in both human and mouse skin, and in cultured keratinocytes and adipocytes. TIP39 was observed in the basal layer of human skin, whereas PTH2R was detected in the spinous to granular layer. The subcellular localization of TIP39 in keratinocytes changed during calcium-induced differentiation and shifted to colocalize with PTH2R at the membrane. The addition of recombinant TIP39 to normal human keratinocytes in culture induced an increase in intercellular calcium and triggered aspects of terminal differentiation including decreased keratin-14 and increased involucrin expression. Consistent with these observations, $PTH2R^{-/-}$ mice were observed to have increased epidermal thickness. In summary, identification of TIP39 and its receptor in the epidermis reveals an additional PTH family member that is expressed in the skin and may influence keratinocyte function.

INTRODUCTION

Vitamin D3 is well known to act with parathyroid hormone (PTH) to regulate calcium and phosphate homeostasis (Strewler, 2000). However, genes related to PTH, such as the PTH-

Correspondence: Richard L. Gallo, Department of Dermatology, University of California San Diego, 9500 Gillman, La Jolla, California 92093, USA. rgallo@ucsd.edu.

CONFLICT OF INTEREST

The authors state no conflicts of interest.

SUPPLEMENTARY MATERIAL

Supplementary material is linked to the online version of the paper at www.jidonline.org, and at http://dx.doi.org/10.1016/j.jid.2016.02.814.

related peptide (PTHrP), have less clearly defined functions. For example, PTHrP has been observed to be expressed in the skin, is extensively post-translationally processed, and has been variously reported to induce both increased and decreased proliferation and differentiation of keratinocytes in vitro (Henderson et al., 1992; Kaiser et al., 1992, 1994). In mice, overexpression of PTHrP in the skin by the keratin-14 (KRT14) promoter led to either a delay or frank failure of hair follicle initiation (Wysolmerski et al., 1994) and also resulted in a thickened ventral epidermis with marked acanthosis and papillomatosis, hyperplastic sebaceous glands, and a cellular dermis (Foley et al., 1998). Conversely, PTHrP-deficient mice die after birth, and exhibited widespread abnormalities of endochondral bone development (Karaplis et al., 1994). Rescue of these mice by expression of PTHrP in cartilage prolongs survival (Philbrick et al., 1998), but the rescued-PTHrP null mice showed a markedly thinned epidermis and striking hyperkeratosis, hypoplastic sebaceous glands, and a fibrotic dermis (Foley et al., 1998).

Tuberoinfundibular peptide of 39 residues (TIP39) is a third member of the PTH ligand family, and an agonist of the PTH second receptor (PTH2R) (Usdin et al., 1999). Human PTH2R shares only 51% amino acid sequence identity with human PTH1R. PTH binds and stimulates both receptors, whereas PTHrP effects on only PTH1R (Usdin et al., 1995). TIP39 also binds to both receptors, but its affinity to the PTH2R a hundredfold stronger than to PTH1R. Exogenous TIP39 has an antagonistic activity on PTH1R (Hansen et al., 2002; Hoare et al., 2000).

The functions of TIP39 and PTH2R are incompletely understood. In contrast to the severe phenotype seen in PTHrP$^{-/-}$mice, TIP39-deficient mice do not die in the early postnatal period but are sterile because they lack proper maturation of spermatogenic cells (Usdin et al., 2008). Overexpression of human PTH2R produced a dose-dependent inhibition of human embryonic kidney cell proliferation (Misiano et al., 2003). TIP39/PTH2R signaling also has been observed to inhibit the proliferation and alter differentiation of a rat chondrocyte cell line in vitro (Panda et al., 2009). Consistent with this, chondrocyte proliferation was decreased in transgenic mice engineered to overexpress human PTH2R using the Col2a1 promoter (Panda et al., 2012).

Recent work from our lab observed that PTH and PTHrP are important to cutaneous immune defense through the compensation of release of the cathelicidin antimicrobial peptides in the setting of low vitamin D activity (Muehleisen et al., 2012). Because of the profound and unexpected influence of PTH and PTHrP on skin immune function, we sought to gain a more complete understanding of the members of the PTH family in skin. We show here that human and mouse skin express TIP39 and its receptor PTH2R, and show evidence that these molecules may influence skin growth and development.

RESULTS

TIP39 and its receptor PTH2R are expressed in human and mouse skin

To determine if the PTH-related gene *Pth2* (which encodes TIP39 precursor) was expressed in the skin, total RNA was extracted from whole skin and several other tissues of 8-week-old male C57BL/6 mice. Quantitative PCR found that in addition to tissues such as brain and

testis that were known to express TIP39, skin also expressed transcripts for both this gene and its receptor PTH2R (Figure 1a). Protein expression for TIP39 was confirmed by western blot and immunostaining of whole skin (Figure 1b), and demonstrated that this protein was present primarily in the epidermis and dermal adipose layer. Protein extracts from mouse epidermis revealed that TIP39 was processed to three distinct sizes (15–20 kDa, 10–15 kDa, and <10 kDa), whereas mouse white adipose tissue had only a 10–15 kDa band. Each of these peptide processing patterns contrasted with the single 15–20 kDa TIP39 band found in extracts from testis (Figure 1b).

Examination of the pattern of expression of TIP39 by immunohistochemistry showed that this protein was expressed in both mouse and human skin, but localized predominantly in the spinous layer of mouse epidermis and mostly in the basal layer of human skin (Figure 1c). In contrast, PTH2 receptor expression was seen in an alternative pattern, with high expression in basal keratinocytes of mice and expression predominantly in the spinous to granular layer of humans (Figure 1c).

We next investigated the expression of TIP39 and PTH2R during the development of hair in the early postnatal period, and in skin cell types other than keratinocytes. Dorsal skin from mouse postnatal day 2 to day 10 (P2–P10) was collected to represent hair cycle in anagen, from P16 to P19 to represent catagen, and from P20 to P21 to represent telogen (Ma et al., 2003; Muller-Rover et al., 2001; Paus, 1998; Plikus and Chuong, 2008; Runkel et al., 2012). Both *Pth2* and *Pth2r* gene expressions were increased in catagen and suppressed in early anagen and late telogen (Supplementary Figure S1a online). Adipocytes in culture also showed a change in TIP39 during differentiation with TIP39 protein increased during maturation from preadipocyte to adipocytes (Supplementary Figure S1b). PTH2R mRNA was also detectable in these cells (data not shown). The expression of this protein was confirmed by detection of appropriately sized bands by western blot of skin extracts (Supplementary Figure S1c). Furthermore, the specificity of immunohistochemistry was confirmed by the loss of signal on the addition of excess blocking peptide or the absence of signal when staining skin from TIP39$^{-/-}$mice (Supplementary Figure S1c–e). TIP39 did not colocalize with major histocompatibility complex class 2 expressing Langerhans cells (Supplementary Figure S1f). Taken together, these observations demonstrated that TIP39 and PTH2R are present in skin, expressed by keratinocytes and adipocytes, and are detectable in a strictly controlled pattern of expression that may be different between humans and mice.

Expression of TIP39 and PTH2R changes during differentiation

The expression patterns of TIP39 and its receptor suggested that the function of this gene in the skin may be related to keratinocyte differentiation. TIP39 and PTH2R were therefore examined in normal human epidermal keratinocytes (NHEK) in vitro undergoing calcium (Ca^{2+})-induced differentiation (Boyce and Ham, 1983). Western blots of extracts from three-dimensional epidermal constructs showed the appearance of multiple TIP39 bands in these cells (Figure 2a), but no change in mRNA expression (Supplementary Figure S2a online). In adipocytes undergoing differentiation, TIP39 bands were also observed to change size (Supplementary Figure S1b). Lysates from low and high calcium-cultured keratinocytes also

detected PTH2R and showed an increase in band intensity during differentiation (Figure 2b) and mRNA of PTH2R was also increased (Supplementary Figure S2a).

Immunohistochemistry showed that under basal growth conditions of low Ca^{2+}(0.06 mM), both TIP39 and PTH2R localized in NHEK in a perinuclear pattern, and then shifted to the plasma membrane when differentiated by 1.2 mM Ca^{2+} (Figure 2c and d). To clarify the location of PTH2R in NHEK, cells were permeabilized by Triton X-100 (Lorenz et al., 2006; Roosterman et al., 2006; Stadler et al., 2010) and compared with cells fixed by 4% paraformaldehyde without Triton X-100. Triton X-100 solubilized receptors from the surface and reduced PTH2R staining on calcium-differentiated NHEK (Supplementary Figure S2b). However, permeabilization enhanced cytosolic access of the antibody and increased staining of intracellular PTH2R. These data suggested that PTH2R localized predominantly in the cytosol of proliferative keratinocytes, whereas differentiation induced a shift of PTH2R to the plasma membrane. As a negative control to demonstrate specificity of the antibody, A431 cells that showed low PTH2R expression by western blot were seen to have negative immunofluorescence (Supplementary Figure S2c and d).

TIP39 binds to PTH2R on endoplasmic reticulum

To begin to understand the potential functions of TIP39 in keratinocytes, we next evaluated the response of NHEK to the addition of synthetic TIP39 peptide to culture media. Five minutes after the addition of the TIP39 peptide, PTH2R shifted from the perinuclear zone to the plasma membrane in a pattern similar to that seen on the addition of the calcium to the culture media. Use of rhodamine-labeled TIP39 demonstrated that the exogenously added peptide colocalized with its receptor (Figure 3a). Furthermore, exogenous TIP39 also colocalized with an endoplasmic reticulum (ER) molecular probe and calnexin (Figure 3b, Supplementary Figure S2e and g) and only partially colocalized with a Golgi molecular probe (Supplementary Figure S2f and g).

Next, we analyzed the global gene expression profiles of TIP39-stimulated NHEK using RNA sequencing. Gene ontology analysis revealed that ER-related categories were the top of differentially enriched gene sets in NHEK after the addition of TIP39. Furthermore, ion transport categories were also highly represented in the differentially enriched gene, together with “phosphatidylinositol-3,5-bisphosphate binding” and “negative regulation of endoplasmic reticulum calcium ion concentration” gene ontology terms (Figure 3c). These results suggested that exogenous TIP39 may influence calcium ion homeostasis in NHEK and prompted us to next measure intracellular calcium ($[Ca^{2+}]i$) in keratinocytes.

TIP39 increases $[Ca^{2+}]i$ of keratinocytes

Figure 3c suggested exogenous TIP39 influenced expression of genes involved in protein localization to the ER and regulates ion transport activity under conditions of low extracellular calcium. Under basal growth conditions containing low concentrations of calcium in the medium, TIP39 increased $[Ca^{2+}]i$ in a dose-dependent manner (Figure 4a). Next, we decreased PTH2R expression by shRNA (Figure 4b, Supplementary Figure S2g) and observed that PTH2R knockdown inhibited upregulation of $[Ca^{2+}]i$ in response to TIP39 (Figure 4c and d). These data suggest that TIP39 increases $[Ca^{2+}]i$ via PTH2R, and regulates

calcium homeostasis in low extracellular calcium conditions. Furthermore, pretreatment with inhibitors of the IP3 pathway, such as calmodulin, phospholipase C, and inositol 1,4,5-trisphosphate receptors, reduced the effects of TIP39 from 17.8% to 5.7%, 6.0%, and 7.1%, respectively (Figure 4e, lower graphs), but the inhibitor of nicotinic acid adenine dinucleotide phosphate that targets acidic endolysosomal Ca^{2+} stores (Park et al., 2015) and sarcoplasmic/endoplasmic reticulum Ca^{2+} ATPase did not effectively block the TIP39 response (12.2% and 13.6%, respectively) (Figure 4e, upper-right two graphs).

TIP39 influences keratinocyte growth and differentiation

Consistent with the effects of TIP39 on calcium homeostasis, a change of morphology was apparent in NHEK exposed to TIP39 for 120 hours (Figure 5a). TIP39 also induced a dose-dependent change in NHEK proliferation as determined by proliferating cell nuclear antigen (PCNA) staining (Figure 5b) and Ki67 expression, a decrease in KRT14 expression, and an increase in involucrin (Figure 5b and c). TIP39 also resulted in a decrease in the expression of the cathelicidin antimicrobial peptide gene (Figure 5d). This effect was opposite to that previously observed to be induced by PTH or PTHrP (Muehleisen et al., 2012). The addition of the PTH2R antagonist (HYWH) blocked the effects of TIP39 on these genes and supported the conclusion that these effects of TIP39 were specific to the interaction with PTH2R (Figure 5e).

Next, three-dimensional skin constructs were exposed to TIP39 to determine the response of keratinocytes in an epidermal model more reflective of the epidermis in vivo. In these three-dimensional skin constructs, exogenous TIP39 decreased the thickness of the KRT14 positive layer and increased staining for the terminal differentiation marker filaggrin (FLG) (Figure 5f). mRNA expression for KRT14 and FLG showed a similar trend after exposure to TIP39 (Figure 5g).

Finally, we evaluated the skin of 10- to 13-week-old female $PTH2R^{-/-}$mice and their littermates. Consistent with the effects of TIP39 to slow keratinocyte growth and induce differentiation, the epidermis of $PTH2R^{-/-}$mice was observed to be thicker than their littermates (Figure 6a and b). KRT14 staining was increased in $PTH2R^{-/-}$epidermis, and accordingly, FLG expression was suppressed (Figure 6c and d). p63 and PCNA staining were also more frequently seen in keratinocytes from the $PTH2R^{-/-}$epidermis than littermate controls (Figure 6e and f). Taken together, these findings suggest that TIP39 activation of PTH2R can influence keratinocytes differentiation.

DISCUSSION

In this study, we observed that TIP39 and its receptor PTH2R are expressed in the skin and that their presence may be a previously unknown system to influence keratinocyte calcium homeostasis and differentiation. The work was motivated by prior observations of the influence of another PTH1R on keratinocyte antimicrobial peptide expression and the capacity of the skin to resist infections (Muehleisen et al., 2012). Therefore, to better understand how other PTH-related hormones may affect skin biology we evaluated the expression of PTH2R and TIP39, members of the PTH family that had not been studied in skin. We found for the first time to our knowledge that TIP39-PTH2R was expressed in the

epidermis and we present several observations that associate the expression of TIP39 or PTH2R with keratinocyte calcium homeostasis and differentiation. These findings provide insight into the complex systems by which PTH-related genes can regulate skin behaviors.

The expression of TIP39 in skin was detected by multiple approaches in this study, including quantitative PCR, immunostaining, and western blot of tissue and cell extracts. The predominant cell types of the skin that expressed TIP39 were keratinocytes and adipocytes, but it is possible that other cell types, particularly neural elements in the skin, may also express these molecules. Interestingly, although proliferative keratinocytes and preadipocytes predominantly expressed TIP39 in the larger 15–20 kDa precursor form, differentiation induced processing to smaller forms in both cell types (Figure 2a, Supplementary Figure S1b). Those data suggest that differentiation triggers post-translational modification of PTH2/TIP39, possibly to result in generation of the actual 39-residue peptide and activation of function. Future experiments to include more precise mass and sequence determinations will be necessary to clearly identify if the antigen detected by immunostaining is indeed the TIP39 peptide.

The staining pattern of TIP39 in the epidermis showed a striking difference between normal human and mouse skin. It is unclear why this pattern differed between species, but cultured human keratinocytes showed a pattern of expression during differentiation similar to what was seen in vivo, namely a perinuclear pattern in undifferentiated basal cells and a plasma membrane pattern in differentiated cells. Differences between mice and human expression patterns may reflect one of many fundamental differences between mouse and human skin or be simply due to difficulties in accurate localization techniques in the thin murine epidermis. Furthermore, preliminary observations of skin tumors also suggested that TIP39 expression changes in transformed keratinocytes and reflects their final state of differentiation. Basal cell carcinomas showed abundant perinuclear staining, whereas squamous cell carcinomas had much lower staining (data not shown).

The presence of TIP39 in the skin is likely to be functionally relevant. Exogenous TIP39 colocalized with PTH2R at the ER (Figure 3a and b). Currently, it is not clear how TIP39 entered the cell. Although PTH and PTHrP bind to PTH1R on the plasma membrane and these complexes enter by endocytosis, PTH2R was only weakly detectable on the plasma membrane in our study. This low level of expression may be sufficient for entry, or TIP39 may enter using other ER-shuttling mechanisms. Support for alternative entry mechanisms can be seen from observations that anoctamin-1, a calcium activated chloride channel, complexes with G protein-coupled receptors such as bradykinin receptor 2, and then the plasma membrane component of the complex is tethered to the ER via the interaction of anoctamin-1 with inositol 1,4,5-triphosphate receptor 1 (Jin et al., 2013). Indeed, we observed that expression of some calcium activated chloride channel genes was significantly changed by the addition of TIP39 (Figure 3c, Supplementary Table S1 online).

An important observation from the current study is that the addition of TIP39 to NHEK increased $[Ca^{2+}]i$ (Figure 4). Increased cytosolic calcium was associated with an expected increase in keratinocyte differentiation (Figure 5). Although the response of $[Ca^{2+}]i$ required relatively high amounts of TIP39, the effect of the peptide appeared specific as it was

dependent on its receptor. PTH2R knockdown reduced the short-term effects of TIP39 on $[Ca^{2+}]i$ (Figure 4d). In the case of p1 NHEK, 10 μM TIP39 increased $[Ca^{2+}]i$ 17.8% compared with the control group (Figure 4e, upper left). The pretreatment of inhibitors of inositol 1,4,5-trisphosphate receptors, phospholipase C, and calmodulin reduced the effects of TIP39 (Figure 4e, lower graphs). Inhibitors of sarcoplasmic/endoplasmic reticulum Ca^{2+} ATPase and nicotinic acid adenine dinucleotide phosphate did not inhibit TIP39 responses compared with those inhibitors (Figure 4e, upper-right two graphs). Thapsigargin and bafilomycin A also slightly reduced the response of TIP39. These data suggest that the IP3 pathway is an important pathway of the TIP39 response. Furthermore, the PTH2R antagonist HYWH-TIP39 partially reversed the effects of TIP39 on differentiation (Figure 5e). These data suggest that TIP39 interacts with PTH2R, and that receptor-dependent and -independent events are likely involved in the action of TIP39 on epidermal differentiation. Indeed, the altered phenotype of the epidermis in $PTH2R^{-/-}$mice further supported the biological relevance of the receptor-dependent effects. Future studies of the complex mechanism of action of the PTH-related genes in the skin will be needed to better understand the relative role of TIP39.

In addition to the data presented herein, a review of the existing literature on the mechanisms of action of PTH offers insight into why these genes are important to the skin. The parathyroid gland responds to changes in the level of calcium in the blood by the secretion of PTH. Circulating PTH works to increase blood calcium levels by stimulating osteoclastic bone reabsorption to release calcium and phosphate (DiGirolamo et al., 2012). PTH is not detectable in the skin, but calcium homeostasis is an essential aspect of normal epidermal function and is critical in regulation of keratinocyte differentiation. TIP39 and PTH2R may assume this role in the epidermis. Previously, it was shown that PTH2R responds to increases of $[Ca^{2+}]i$ concentration and inositol phosphates in response to PTH (Behar et al., 1996). However, TIP39 is a stronger agonist than PTH for increasing $[Ca^{2+}]i$ concentration via the PTH2R (Della Penna et al., 2003; Goold et al., 2001). Therefore, our observations of an increase in calcium in the cytosol of keratinocytes after exposure to TIP39, and changes in keratinocyte morphology and gene expression on deletion of PTH2R, make it tempting to speculate that TIP39 and PTH2R are previously unrecognized mechanisms for control of keratinocyte calcium homeostasis. Future work will directly examine these events.

In summary, this study demonstrates that the unique PTH-related gene *PTH2*/TIP39 and its receptor PTH2R are expressed in the skin. The functions of these genes in cutaneous biology are different from PTHrP or PTH1R, and likely involve mechanisms that regulate keratinocyte differentiation and calcium transport. These molecules may also play a role in genetic skin disorders involving abnormal calcium transport such as Darier disease or Hailey-Hailey disease.

MATERIALS AND METHODS

Cells and reagents

NHEK were cultured as previously described (MacLeod et al., 2015; Morizane et al., 2010; Yamasaki et al., 2011). Cells at 70% to 80% confluence were stimulated with 0.06 mM or

1.2 mM $CaCl_2$ (Life Technologies, NY) from 12 hours to 120 hours. Three-dimensional in vitro skin constructs were prepared as described (Borkowski et al., 2013). TIP39 peptides (10–1000 nM; Bachem Americas, Torrance, CA; Phoenix Pharmaceuticals, Burlingame, CA), HYWH-TIP39 peptides (0.1–10 μM; gift from Dr Usdin, NIMH, MD), or control (phosphate buffered saline) was added in culture media from 24 to 120 hours. All culture media and chemicals were replaced every other day.

Mice

Male C57BL/6 mice (8–12 weeks) were housed at the University Research Center at the University of California, San Diego. Skins of female PTH2R and TIP39 knockout mice (10–13 weeks) were a gift of Dr Usdin (NIMH). All animal experiments were approved by the UCSD (University of California, San Diego) Institutional Animal Care and Use Committee.

Isolation of total RNA and quantitative reverse transcriptase-PCR

Total RNA from skin samples and cultured keratinocytes was extracted, and cDNA was synthesized as previously described (Morizane et al., 2012; Muto et al., 2014; Yamasaki et al., 2009). TaqMan Gene Expression Assays (Applied Biosystems ABI, Foster City, CA) were used to analyze expressions of mouse TIP39 (assay ID: Mm01202460_g1), mouse PTH2R (assay ID: Mm01257118_m1), human Ki67 (assay ID: Hs01032443_m1), human KRT14 (assay ID: Hs00265033_m1), and human involucrin (assay ID: Hs00846307_s1) as described by the manufacturer's instructions. Human glyceraldehyde-3-phosphate dehydrogenase (GAPDH) (assay ID: Hs02758991_g1) or mouse β-actin (assay ID: Mm00607939_s1) was used as an internal control to validate RNA for each sample. Primers sequence of human TIP39, PTH2R or GAPDH are described in Supplementary Table S2 online. Each mRNA expression was calculated as the relative expression to glyceraldehyde-3-phosphate dehydrogenase or b-actin mRNA, and all data are presented as a fold change against each control (mean of nonstimulated cells).

RNA sequence

RNA quality was checked using the R6K screen tape with an Agilent 2200 TapeStation (Agilent Technologies, Santa Clara, CA). RNA-sequence libraries were prepared using the TruSeq Stranded mRNA (Illumina, San Diego, CA) and sequenced with the HiSeq2500, HighOutput v4 system (Illumina). All those processes were performed at the IGM (Institute for Genomic Medicine) Genomics Center, University of California, San Diego, La Jolla, CA. The gene expression level was quantified by the number of uniquely mapped reads per kilobase of exon per million mapped reads. Gene ontology analysis, hierarchical clustering, and heat map generation were performed with the Partek Flow. Significantly enriched gene ontology functional groups were defined as having an enrichment score less than P-value < 0.05, and each functional group was assigned with a gene ontology enrichment score calculated using Fisher's exact test.

Lentiviral shRNA transduction to NHEK

PTH2R and control shRNA lentiviral particles were purchased from Santa Cruz Biotechnology (Dallas, TX). Lentivirus transduction was performed by the manufacturer's

instructions and previous report (Sato et al., 2013). Puromycin (5 μg/ml) is used for 6-week selection.

Western blot

Protein isolation and transfer were performed as previously described (MacLeod et al., 2013; Yamasaki et al., 2006). Anti-TIP39 (1 μg/ml; Santa Cruz, CA or Fitzgerald, MA), anti-PTHrP (1 mg/ml; Santa Cruz), anti-PTH2R (0.4 μg/ml; gift from Dr Usdin, NIMH), anti-glyceraldehyde-3-phosphate dehydrogenase (1 μg/ml; Fitzgerald), and antiβactin (1 μg/ml; Sigma-Aldrich, MO) antibodies were used for protein detection. IR-dye conjugated secondary antibodies (680 and 800 nm; 1:10,000) and an Odyssey imager and quantification software (LI-COR Biosciences, Lincoln, NE) were used for two-color western blotting to analyze both proteins on the same blot.

Immunofluorescence staining of cultured cells

Cells were fixed in −20°C cold methanol for 10 minutes and then blocked with phosphate buffered saline containing 5% donkey serum at room temperature for 30 minutes. Immunostaining was performed by the manufacturer's instructions (CST, Immunofluorescence General Protocol of IF-IC). Anti-TIP39, anti-PTH2R, anti-E-cadherin (CST, MA), anti-PCNA (CST), secondary Alexa Fluor 488 or 594-conjugated antibodies (Life Technologies) were used at 1 μg/ml. ER-ID Green dye (Enzo Life Sciences, NY) is used for endoplasmic reticulum staining by the manufacturer's protocol. Cover slips were mounted using ProLong Gold antifade reagent with 4′,6-diamidino-2-phenylindole (Life Technologies). Images were captured using a BX41 microscope (Olympus, Center Valley, PA).

Immunofluorescence for paraffin-embedded sections

Immunostaining was performed by the manufacturer's instructions (CST, Immunofluorescence General Protocol of IF-P). The skin tissue samples were fixed in 10% formalin for 24 hours. Five-micron paraffin sections were deparaffinized and rehydrated before heat-induced antigen retrieval was performed in 10 mM citrate buffer (pH 6.0). Anti-TIP39, anti-PTH2R, anti-Keratin14 (Santa Cruz), anti-FLG, anti-p63 (Thermo Scientific, IL), anti-PCNA (CST), secondary Alexa Fluor 488, or 594-conjugated antibodies (Life technologies) were used at 1 μg/ml. Epidermal thickness, FLG positive area, and PCNA positive cells were calculated as in previous reports (Gonzalez et al., 2003; Marsella et al., 2013).

$[Ca^{2+}]i$ measurements

$[Ca^{2+}]i$ was measured by a Fluo-4 NW Calcium Assay Kit (Life Technologies). Because the calcium ion concentration of the NHEK culture medium is low, we used low calcium contained-balanced salt solution (10 mM HEPES, pH7.4, 120 mM NaCl, 4 mM KCl, 1 mM KH_2PO_4, 1 mM $MgCl_2$, 5 mM glucose, and 0.05 mM $CaCl_2$) (Karvonen et al., 2000) instead of the Kit-included Assay buffer. To study calcium ion influx, cells were incubated with dye loading solution (balanced salt solution with Fluo-4 NW dye mix and 2.5 mM probenecid) at 37°C for 30 minutes, and then at room temperature for an additional 30 minutes. TIP39

peptide (5–25 μM), ionomycin (1 μM), thapsigargin (1 μM) (Enzo Life Science), bafilomycin A (0.5 μM) (Sigma-Aldrich), xestospongin C (5 μM), U73122 (5 μM), and W-7 (50 μM) (TOCRIS Bioscience, Bristol, UK) were added as indicated in dye loading solution, and then $[Ca^{2+}]i$ was monitored at an emission of 516 nm with excitation of 494 nm using a SpectraMax Gemini EM microplate Reader (Molecular Devices, Sunnyvale, CA) (Jiang et al., 2011). Fluo-4 signal changes (%) were defined as (F − F0)/F0 × 100. F was the target fluorescence signal intensity and F0 was the baseline calculated by averaging five time points just before the application of the stimulus.

Statistical analysis

Data are expressed as means ± SEM. Differences between experimental groups within each experiment were analyzed using the unpaired Student t-test and were considered significant at $P \leq 0.05$.

Supplementary Material

Refer to Web version on PubMed Central for supplementary material.

Acknowledgments

This work was supported in part by NIH grants R01AI116576, R01AR064781, R01AI052453, R21AR0675478, U19AI117673, and P01HL107150 (RLG) and the UCSD Dermatologist Investigator Training Program T32AR062496 (JAS, CA).

Abbreviations

Ca^{2+}	calcium
$[Ca^{2+}]i$	intracellular calcium
ER	endoplasmic reticulum
FLG	filaggrin
KRT14	keratin-14
NHEK	normal human epidermal keratinocytes
PCNA	proliferating cell nuclear antigen
PTH	parathyroid hormone
PTHrP	PTH-related peptide
PTH2R	PTH second receptor
TIP39	tuberoinfundibular peptide of 39 residues

References

Behar V, Pines M, Nakamoto C, Greenberg Z, Bisello A, Stueckle SM, et al. The human PTH2 receptor: binding and signal transduction properties of the stably expressed recombinant receptor. Endocrinology. 1996; 137:2748–57. [PubMed: 8770894]

Borkowski AW, Park K, Uchida Y, Gallo RL. Activation of TLR3 in keratinocytes increases expression of genes involved in formation of the epidermis, lipid accumulation, and epidermal organelles. J Invest Dermatol. 2013; 133:2031–40. [PubMed: 23353987]

Boyce ST, Ham RG. Calcium-regulated differentiation of normal human epidermal keratinocytes in chemically defined clonal culture and serum-free serial culture. J Invest Dermatol. 1983; 81:33s–40s. [PubMed: 6345690]

Della Penna K, Kinose F, Sun H, Koblan KS, Wang H. Tuberoinfundibular peptide of 39 residues (TIP39): molecular structure and activity for parathyroid hormone 2 receptor. Neuropharmacology. 2003; 44:141–53. [PubMed: 12559132]

DiGirolamo DJ, Clemens TL, Kousteni S. The skeleton as an endocrine organ. Nat Rev Rheumatol. 2012; 8:674–83. [PubMed: 23045255]

Foley J, Longely BJ, Wysolmerski JJ, Dreyer BE, Broadus AE, Philbrick WM. PTHrP regulates epidermal differentiation in adult mice. J Invest Dermatol. 1998; 111:1122–8. [PubMed: 9856827]

Gonzalez S, Astner S, An W, Goukassian D, Pathak MA. Dietary lutein/zeaxanthin decreases ultraviolet B-induced epidermal hyperproliferation and acute inflammation in hairless mice. J Invest Dermatol. 2003; 121:399–405. [PubMed: 12880433]

Goold CP, Usdin TB, Hoare SR. Regions in rat and human parathyroid hormone (PTH) 2 receptors controlling receptor interaction with PTH and with antagonist ligands. J Pharmacol Exp Ther. 2001; 299:678–90. [PubMed: 11602681]

Hansen IA, Jakob O, Wortmann S, Arzberger T, Allolio B, Blind E. Characterization of the human and mouse genes encoding the tuberoinfundibular peptide of 39 residues, a ligand of the parathyroid hormone receptor family. J Endocrinol. 2002; 174:95–102. [PubMed: 12098667]

Henderson JE, Kremer R, Rhim JS, Goltzman D. Identification and functional characterization of adenylate cyclase-linked receptors for parathyroid hormone-like peptides on immortalized human keratinocytes. Endocrinology. 1992; 130:449–57. [PubMed: 1309343]

Hoare SR, Clark JA, Usdin TB. Molecular determinants of tuberoinfundibular peptide of 39 residues (TIP39) selectivity for the parathyroid hormone-2 (PTH2) receptor. N-terminal truncation of TIP39 reverses PTH2 receptor/PTH1 receptor binding selectivity. J Biol Chem. 2000; 275:27274–83. [PubMed: 10854439]

Jiang Z, Yin X, Jiang Q. Natural forms of vitamin E and 13′-carboxychromanol, a long-chain vitamin E metabolite, inhibit leukotriene generation from stimulated neutrophils by blocking calcium influx and suppressing 5-lipoxygenase activity, respectively. J Immunol. 2011; 186:1173–9. [PubMed: 21169551]

Jin X, Shah S, Liu YN, Zhang HR, Lees M, Fu ZJ, et al. Activation of the Cl^-channel ANO1 by localized calcium signals in nociceptive sensory neurons requires coupling with the IP3 receptor. Sci Signal. 2013; 6:ra73. [PubMed: 23982204]

Kaiser SM, Laneuville P, Bernier SM, Rhim JS, Kremer R, Goltzman D. Enhanced growth of a human keratinocyte cell line induced by antisense RNA for parathyroid hormone-related peptide. J Biol Chem. 1992; 267:13623–8. [PubMed: 1618864]

Kaiser SM, Sebag M, Rhim JS, Kremer R, Goltzman D. Antisense-mediated inhibition of parathyroid hormone-related peptide production in a keratinocyte cell line impedes differentiation. Mol Endocrinol. 1994; 8:139–47. [PubMed: 8170470]

Karaplis AC, Luz A, Glowacki J, Bronson RT, Tybulewicz VL, Kronenberg HM, et al. Lethal skeletal dysplasia from targeted disruption of the parathyroid hormone-related peptide gene. Genes Dev. 1994; 8:277–89. [PubMed: 8314082]

Karvonen SL, Korkiamaki T, Yla-Outinen H, Nissinen M, Teerikangas H, Pummi K, et al. Psoriasis and altered calcium metabolism: downregulated capacitative calcium influx and defective calcium-mediated cell signaling in cultured psoriatic keratinocytes. J Invest Dermatol. 2000; 114:693–700. [PubMed: 10733675]

Lorenz H, Hailey DW, Lippincott-Schwartz J. Fluorescence protease protection of GFP chimeras to reveal protein topology and subcellular localization. Nat Methods. 2006; 3:205–10. [PubMed: 16489338]

Ma L, Liu J, Wu T, Plikus M, Jiang TX, Bi Q, et al. 'Cyclic alopecia' in Msx2 mutants: defects in hair cycling and hair shaft differentiation. Development. 2003; 130:379–89. [PubMed: 12466204]

MacLeod DT, Nakatsuji T, Wang Z, di Nardo A, Gallo RL. Vaccinia Virus Binds to the Scavenger Receptor MARCO on the Surface of Keratinocytes. J Invest Dermatol. 2015; 135:142–50. [PubMed: 25089661]

MacLeod DT, Nakatsuji T, Yamasaki K, Kobzik L, Gallo RL. HSV-1 exploits the innate immune scavenger receptor MARCO to enhance epithelial adsorption and infection. Nat Commun. 2013; 4:1963. [PubMed: 23739639]

Marsella R, Santoro D, Ahrens K, Thomas AL. Investigation of the effect of probiotic exposure on filaggrin expression in an experimental model of canine atopic dermatitis. Vet Dermatol. 2013; 24:260–e57. [PubMed: 23432387]

Misiano P, Scott BB, Scheideler MA, Garnier M. PTH2 receptor-mediated inhibitory effect of parathyroid hormone and TIP39 on cell proliferation. Eur J Pharmacol. 2003; 468:159–66. [PubMed: 12754053]

Morizane S, Yamasaki K, Kabigting FD, Gallo RL. Kallikrein expression and cathelicidin processing are independently controlled in keratinocytes by calcium, vitamin D(3), and retinoic acid. J Invest Dermatol. 2010; 130:1297–306. [PubMed: 20090765]

Morizane S, Yamasaki K, Muhleisen B, Kotol PF, Murakami M, Aoyama Y, et al. Cathelicidin antimicrobial peptide LL-37 in psoriasis enables keratinocyte reactivity against TLR9 ligands. J Invest Dermatol. 2012; 132:135–43. [PubMed: 21850017]

Muehleisen B, Bikle DD, Aguilera C, Burton DW, Sen GL, Deftos LJ, et al. PTH/PTHrP and vitamin D control antimicrobial peptide expression and susceptibility to bacterial skin infection. Sci Transl Med. 2012; 4:135ra166.

Muller-Rover S, Handjiski B, van der Veen C, Eichmuller S, Foitzik K, McKay IA, et al. A comprehensive guide for the accurate classification of murine hair follicles in distinct hair cycle stages. J Invest Dermatol. 2001; 117:3–15. [PubMed: 11442744]

Muto J, Morioka Y, Yamasaki K, Kim M, Garcia A, Carlin AF, et al. Hyaluronan digestion controls DC migration from the skin. J Clin Invest. 2014; 124:1309–19. [PubMed: 24487587]

Panda D, Goltzman D, Juppner H, Karaplis AC. TIP39/parathyroid hormone type 2 receptor signaling is a potent inhibitor of chondrocyte proliferation and differentiation. Am J Physiol Endocrinol Metab. 2009; 297:E1125–36. [PubMed: 19706789]

Panda DK, Goltzman D, Karaplis AC. Defective postnatal endochondral bone development by chondrocyte-specific targeted expression of parathyroid hormone type 2 receptor. Am J Physiol Endocrinol Metab. 2012; 303:E1489–501. [PubMed: 23092913]

Park KH, Kim KN, Park DR, Jang KY, Kim UH. Role of nicotinic acid adenine dinucleotide phosphate (NAADP) in keratinocyte differentiation. J Invest Dermatol. 2015; 135:1692–4. [PubMed: 25668236]

Paus R. Principles of hair cycle control. J Dermatol. 1998; 25:793–802. [PubMed: 9990771]

Philbrick WM, Dreyer BE, Nakchbandi IA, Karaplis AC. Parathyroid hormone-related protein is required for tooth eruption. Proc Natl Acad Sci USA. 1998; 95:11846–51. [PubMed: 9751753]

Plikus MV, Chuong CM. Complex hair cycle domain patterns and regenerative hair waves in living rodents. J Invest Dermatol. 2008; 128:1071–80. [PubMed: 18094733]

Roosterman D, Goerge T, Schneider SW, Bunnett NW, Steinhoff M. Neuronal control of skin function: the skin as a neuroimmunoendocrine organ. Physiol Rev. 2006; 86:1309–79. [PubMed: 17015491]

Runkel F, Hintze M, Griesing S, Michels M, Blanck B, Fukami K, et al. Alopecia in a viable phospholipase C delta 1 and phospholipase C delta 3 double mutant. PLoS One. 2012; 7:e39203. [PubMed: 22723964]

Sato E, Imafuku S, Ishii K, Itoh R, Chou B, Soejima T, et al. Vitamin D-dependent cathelicidin inhibits Mycobacterium marinum infection in human monocytic cells. J Dermatol Sci. 2013; 70:166–72. [PubMed: 23452544]

Stadler C, Skogs M, Brismar H, Uhlen M, Lundberg E. A single fixation protocol for proteome-wide immunofluorescence localization studies. J Proteomics. 2010; 73:1067–78. [PubMed: 19896565]

Strewler GJ. The physiology of parathyroid hormone-related protein. N Engl J Med. 2000; 342:177–85. [PubMed: 10639544]

Usdin TB, Gruber C, Bonner TI. Identification and functional expression of a receptor selectively recognizing parathyroid hormone, the PTH2 receptor. J Biol Chem. 1995; 270:15455–8. [PubMed: 7797535]

Usdin TB, Hoare SR, Wang T, Mezey E, Kowalak JA. TIP39: a new neuropeptide and PTH2-receptor agonist from hypothalamus. Nat Neurosci. 1999; 2:941–3. [PubMed: 10526330]

Usdin TB, Paciga M, Riordan T, Kuo J, Parmelee A, Petukova G, et al. Tuberoinfundibular Peptide of 39 residues is required for germ cell development. Endocrinology. 2008; 149:4292–300. [PubMed: 18483145]

Wysolmerski JJ, Broadus AE, Zhou J, Fuchs E, Milstone LM, Philbrick WM. Overexpression of parathyroid hormone-related protein in the skin of transgenic mice interferes with hair follicle development. Proc Natl Acad Sci USA. 1994; 91:1133–7. [PubMed: 7508121]

Yamasaki K, Kanada K, Macleod DT, Borkowski AW, Morizane S, Nakatsuji T, et al. TLR2 expression is increased in rosacea and stimulates enhanced serine protease production by keratinocytes. J Invest Dermatol. 2011; 131:688–97. [PubMed: 21107351]

Yamasaki K, Muto J, Taylor KR, Cogen AL, Audish D, Bertin J, et al. NLRP3/cryopyrin is necessary for interleukin-1beta (IL-1beta) release in response to hyaluronan, an endogenous trigger of inflammation in response to injury. J Biol Chem. 2009; 284:12762–71. [PubMed: 19258328]

Yamasaki K, Schauber J, Coda A, Lin H, Dorschner RA, Schechter NM, et al. Kallikrein-mediated proteolysis regulates the antimicrobial effects of cathelicidins in skin. Faseb J. 2006; 20:2068–80. [PubMed: 17012259]

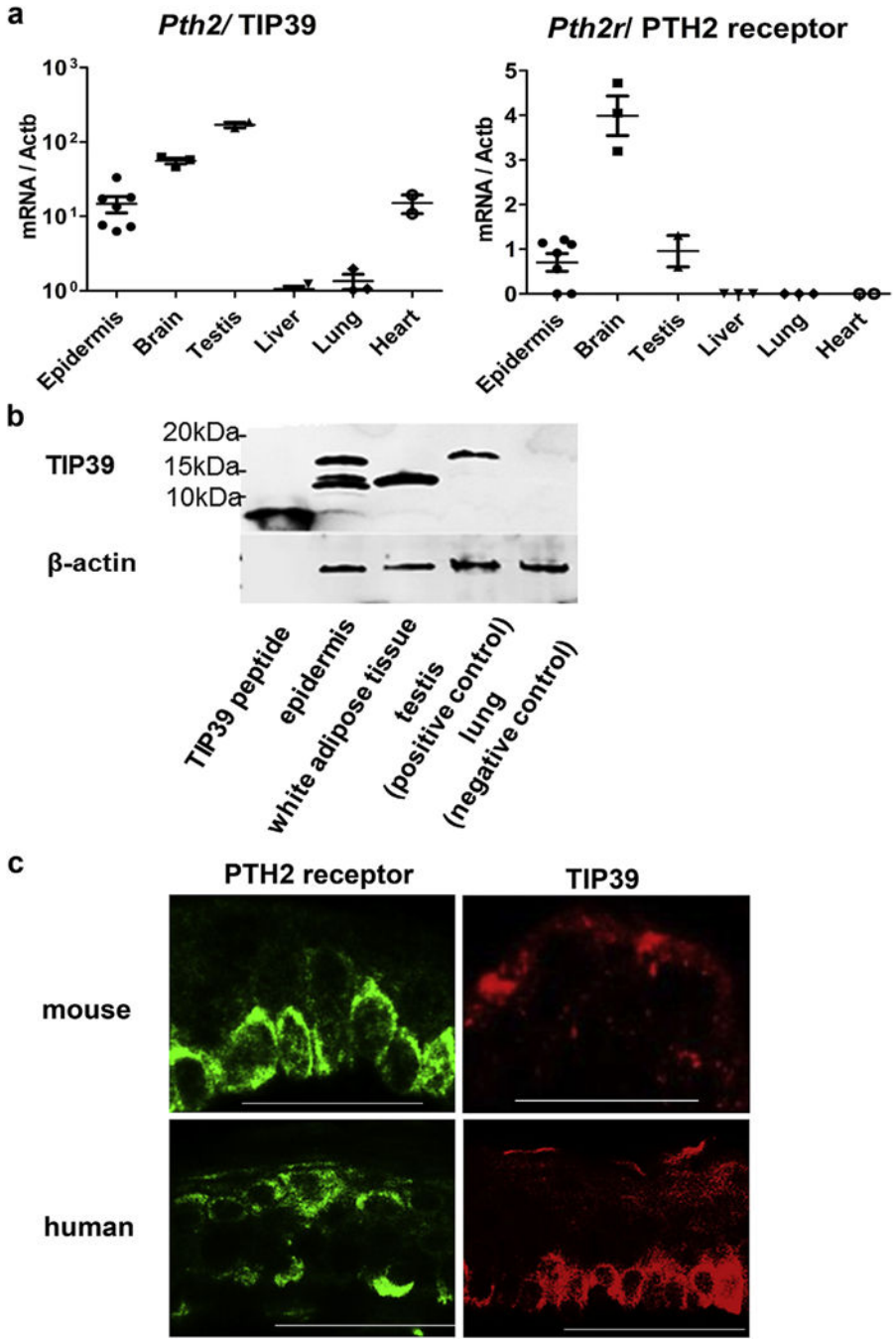

Figure 1. TIP39 and its receptor PTH2 are expressed in human and mouse skin

(**a**) Expression of TIP39 and PTH2R mRNA in tissues isolated from adult C57BL/6 mice. (**b**) Western blot analysis was performed on extracts from mouse tissues (**c**) Human and mouse skin stained for TIP39 (red) or PTH2 receptor (green). Scale bars = 50 μm. PTH2R, PTH second receptor; TIP39, tuberoinfundibular peptide of 39 residues.

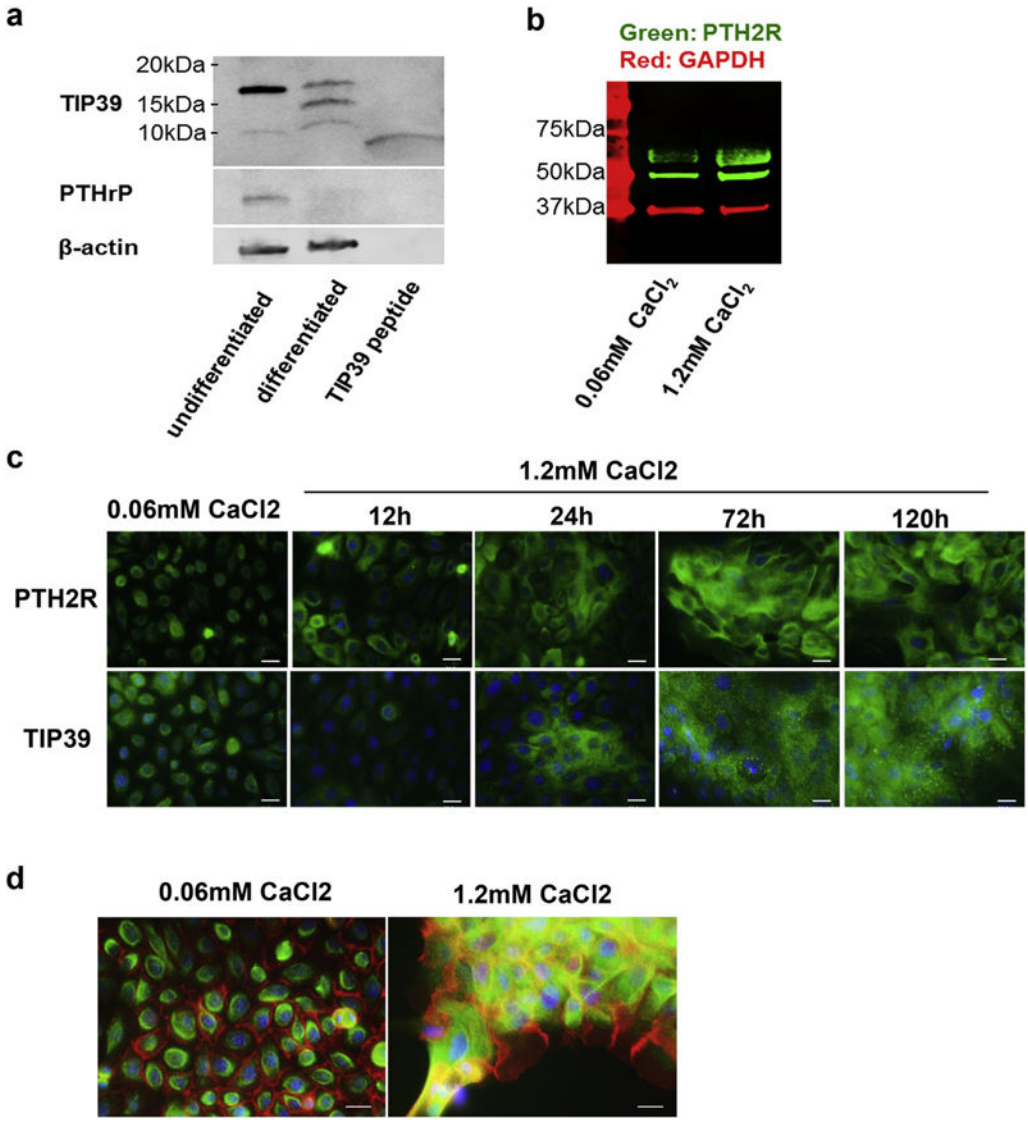

Figure 2. Differentiation associates with a change in the localization of TIP39 and PTH2 receptor in human keratinocytes

(**a**) Western blot of TIP39 and PTHrP in undifferentiated and differentiated normal human keratinocyte lysates. β-Actin is loading control. Differentiated three-dimensional skin constructs were cultured for 25 days. Undifferentiated keratinocytes were incubated in Epilife media with EDGS for 24 hours. (**b**) Western blot of PTH2R in NHEK treated with 0.06 mM or 1.2 mM $CaCl_2$ for 72 hours. GAPDH is a loading control. The predicted size of human PTH2R isoform 1 is 62 kDa, and that of isoform 2 is 50 kDa. (**c**) NHEK were fixed by methanol at 12 hours, 24 hours, 72 hours, and 120 hours after treatment with 1.2 mM $CaCl_2$, and then analyzed by immunofluorescence staining for DAPI (blue) and against TIP39 or PTH2 receptor (green). (**d**) Immunofluorescence staining of PTH2R in NHEK. NHEK cells were treated with 0.06 mM or 1.2 mM $CaCl_2$ for 72 hours. Cells were fixed in ice cold methanol and then analyzed by immunofluorescence staining for DAPI (blue), E-cadherin (red), and PTH2R (green). Scale bars = 20 μm. DAPI, 4′,6-diamidino-2-phenylindole; EDGS, EpiLife Defined Growth Supplement; GAPDH, glyceraldehyde-3-

phosphate dehydrogenase; NHEK, normal human epidermal keratinocytes; PTHrP, PTH-related peptide; PTH2R, PTH second receptor; TIP39, tuberoinfundibular peptide of 39 residues.

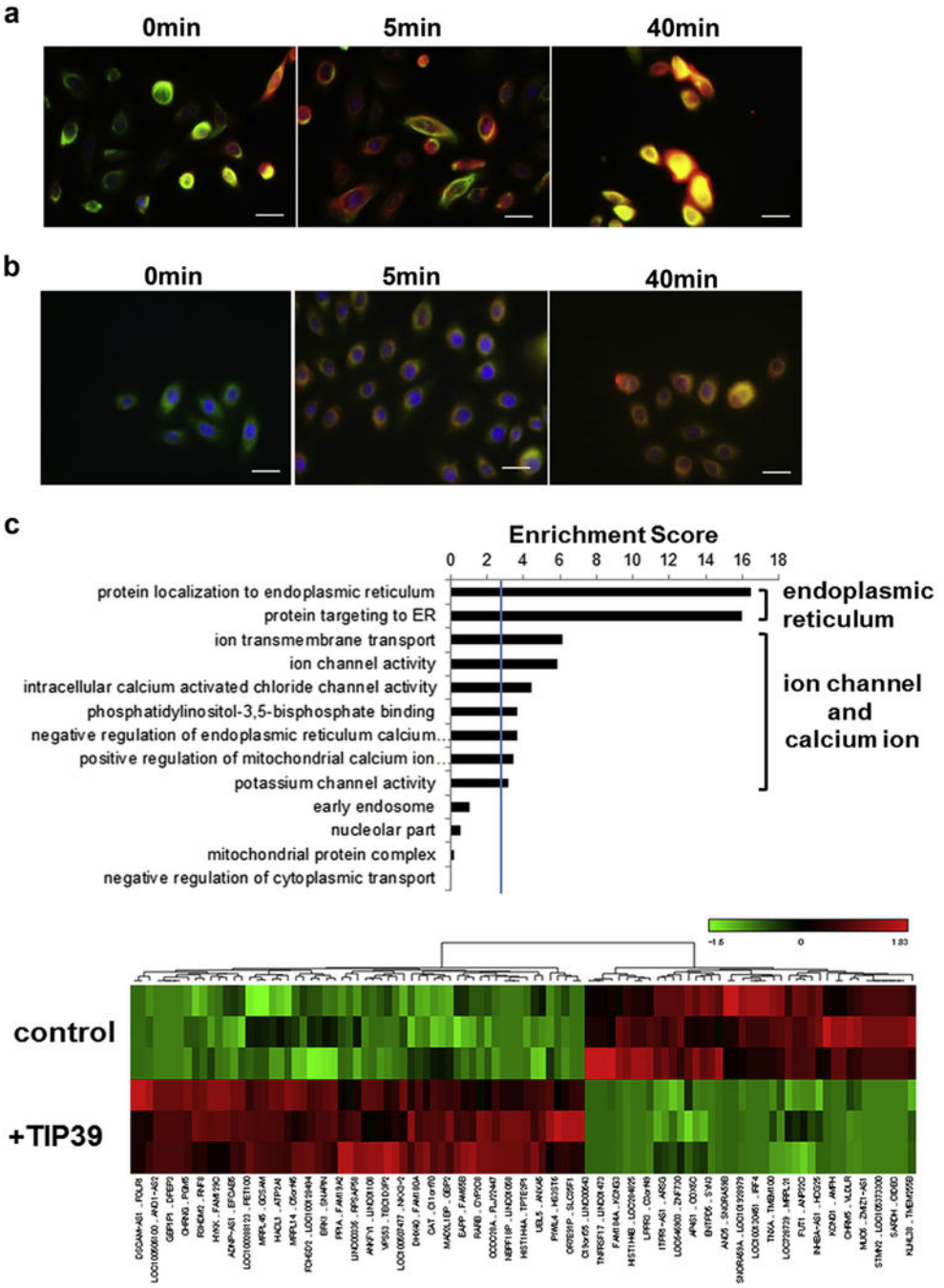

Figure 3. Exogenous TIP39 colocalizes with endoplasmic reticulum and induces a transcriptional response in ER and ion transport gene sets

(**a**) NHEK were treated with 1 μM rhodamine-labeled TIP39 (red). Cells were fixed at 0 minutes, 5 minutes, and 40 minutes after treatment, and then analyzed by immunofluorescence staining for DAPI (blue) and PTH2 receptor (green) or (**b**) endoplasmic reticulum (ER-ID Green dye). Scale bars = 25 μm. (**c**) Gene ontology (GO) analysis and heat map of gene expression in control and 1 μM TIP39-stimulated NHEK samples (n = 3). Green and red indicate down-and upregulated genes, respectively. The blue

line on bar graphs demarks $P = 0.05$. DAPI, 4′,6-diamidino-2-phenylindole; ER, endoplasmic reticulum; NHEK, normal human epidermal keratinocytes; PTH2, PTH second receptor; TIP39, tuberoinfundibular peptide of 39 residues.

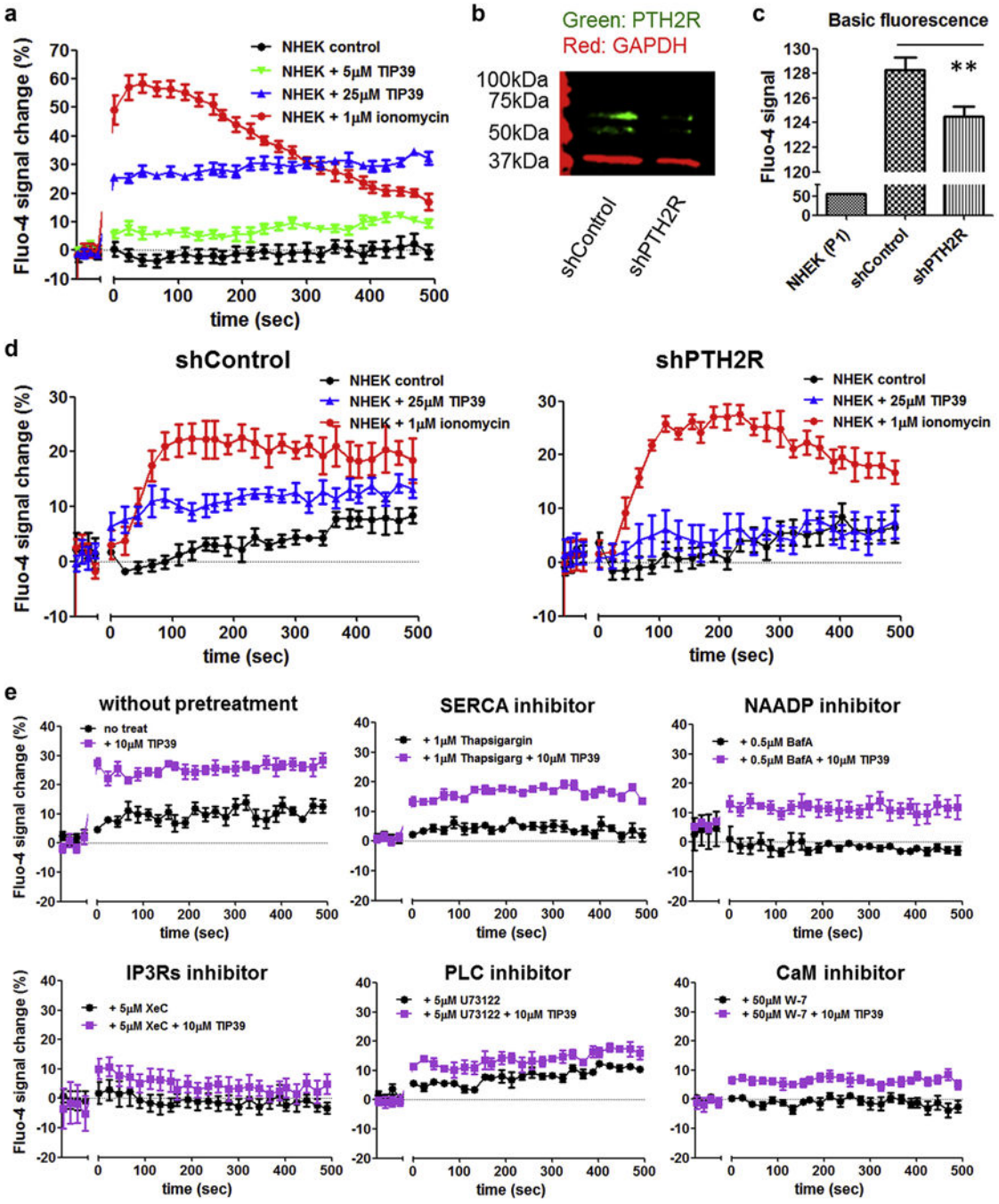

Figure 4. Exogenous TIP39 associates with PTH2R and increases intracellular calcium

(**a**) Intracellular calcium was monitored for 500 seconds after treatment of 5–25 μM TIP39 or 1 μM ionomycin at low concentration (0.05 mM) of$CaCl_2$. (**b**) Western blot of PTH2R in NHEK infected shPTH2R or control lentivirus for 6 weeks. GAPDH is a loading control. (**c**) Basic Fluo-4 fluorescence intensity of untreated NHEK, shControl, and shPTH2R-infected NHEK. (**d**) Intracellular calcium of shPTH2R or shControl lentivirus-infected NHEK was monitored for 500 seconds after treatment of 25 μM TIP39 or 1 μM ionomycin at 0.05 mM of $CaCl_2$. (**e**) NHEK were pretreated for 10 minutes with the following inhibitors: 1 μM

thapsigargin, 0.5 μM bafilomycin A (BafA), 5 μM xestospongin C (XeC), 5 μM U73122 and 50 μM W-7. Intracellular calcium was then monitored for 500 seconds after the addition of 10 μM TIP39 in conditions containing 0.05 mM of $CaCl_2$. $^{**}P < 0.01$. GAPDH, glyceraldehyde-3-phosphate dehydrogenase; NHEK, normal human epidermal keratinocytes; PTH2R, PTH second receptor; TIP39, tuberoinfundibular peptide of 39 residues.

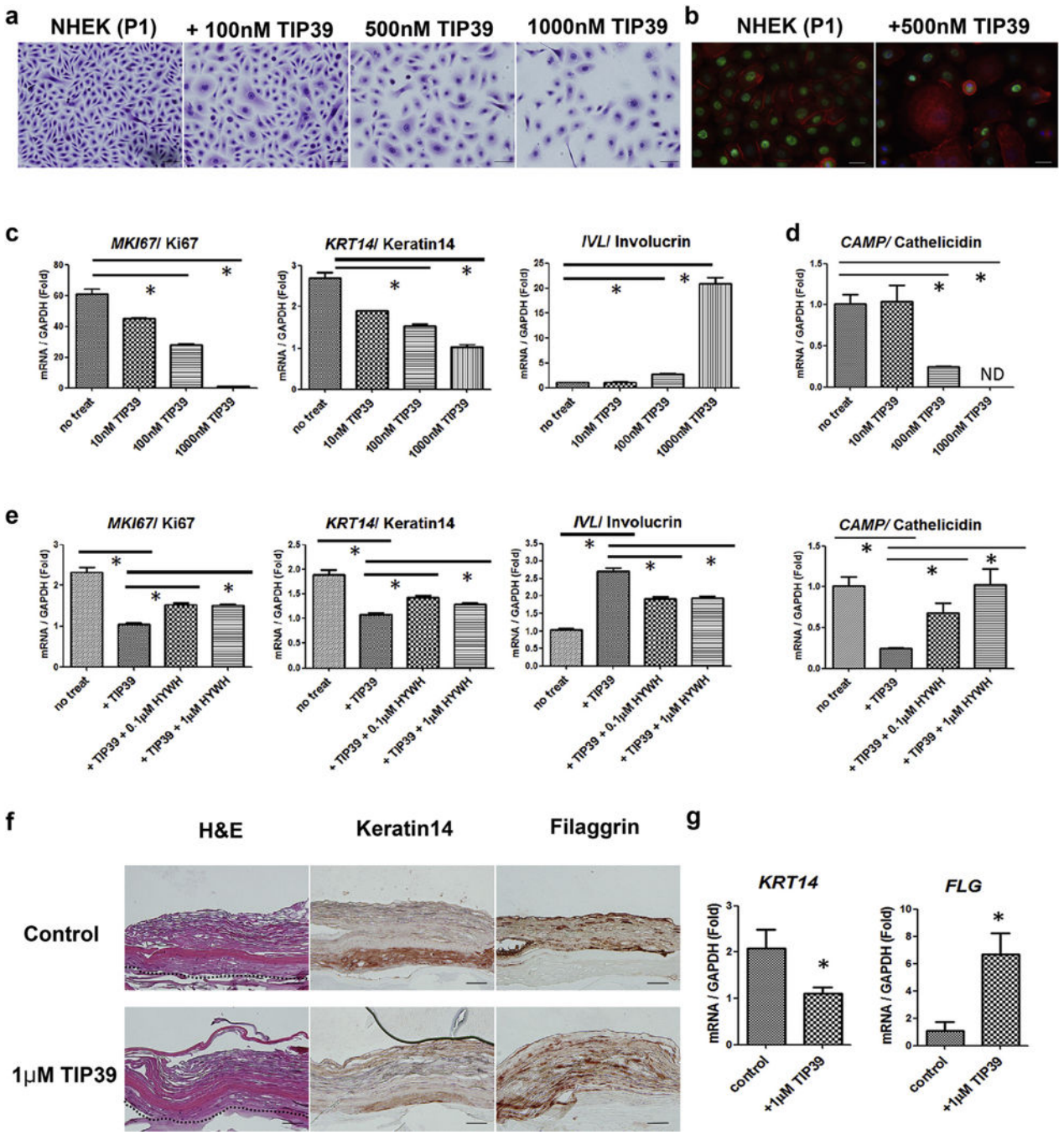

Figure 5. TIP39 alters keratinocyte morphology and expression of differentiation markers

(**a**) NHEK grown under basal (low calcium conditions) were treated with recombinant TIP39 at the indicated doses and then fixed and analyzed by H&E staining 120 hours after treatment. (**b**) Immunofluorescence staining of PCNA in NHEK. NHEK cells were treated with or without 0.5 μM TIP39 for 120 hours. (**c**) NHEK were treated with recombinant TIP39 and then harvested and analyzed by qRT-PCR at 120 hours after treatment. (**d**) NHEK were treated as in (**b**) and analyzed for expression of CAMP mRTA. (**e**) NHEK treated with 1 μM TIP39, 0.1 μM or 1 μM HYWH-TIP39 (HYWH) and then harvested and analyzed by

qRT-PCR at 120 hours after treatment. (**f**) Three-dimensional skin constructs were treated with vehicle or 1 μM TIP39 and then fixed and analyzed by H&E staining and immunohistochemistry at 48 hours after treatment. Scale bars = 50 μm. (**g**) mRNA expression of *KRT14* and *FLG* in the three-dimensional skin construct. Data are means ± SEM, n = 3. **P* < 0.05. FLG, filaggrin; H&E, hematoxylin and eosin; NHEK, normal human epidermal keratinocytes; PCNA, proliferating cell nuclear antigen; qRT-PCR, quantitative reverse transcriptase-PCR; TIP39, tuberoinfundibular peptide of 39 residues.

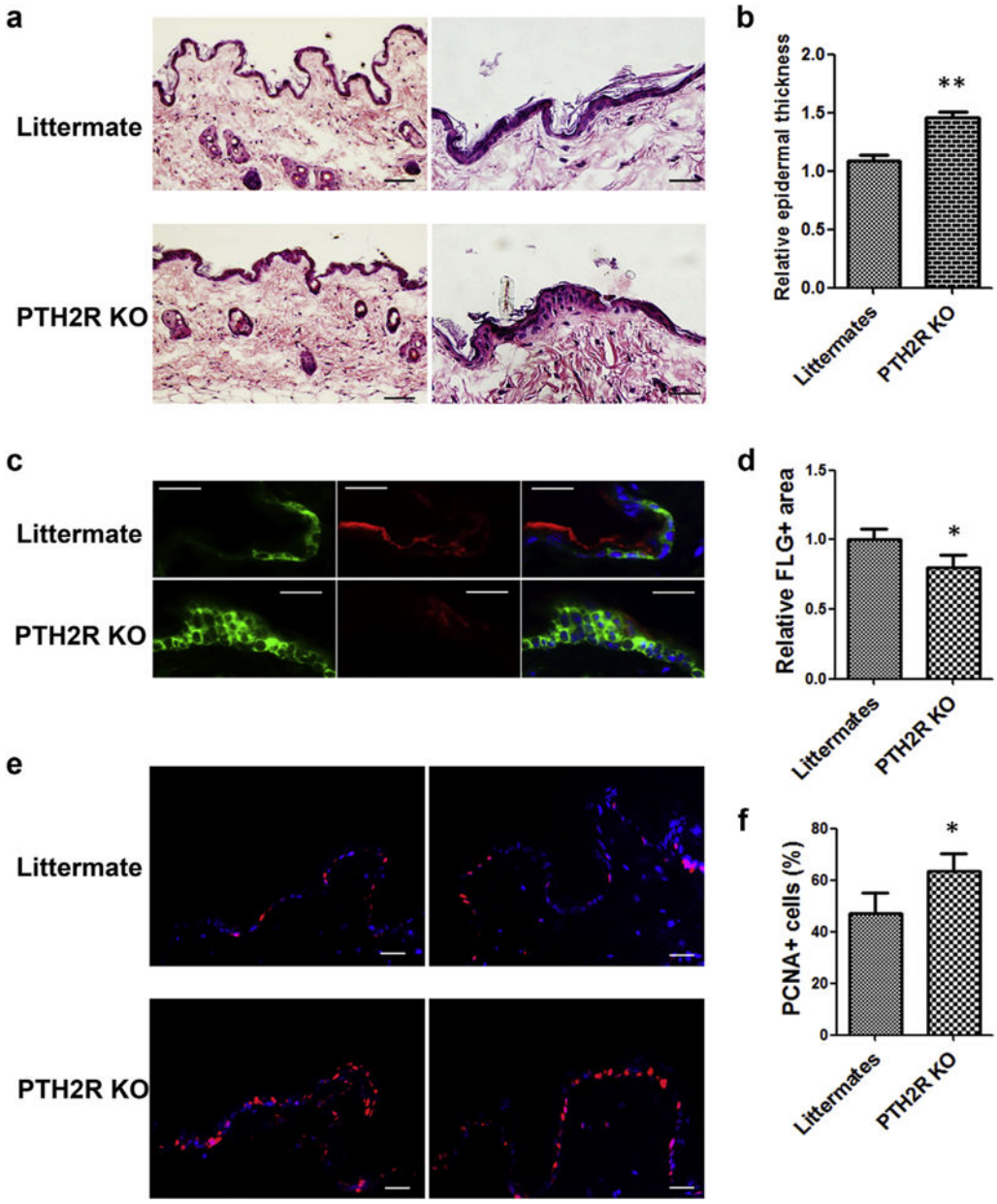

Figure 6. PTH2R knockout mouse epidermis shows evidence of delayed differentiation

(**a**) H&E staining of the skin of PTH2 receptor knockout mouse or wild-type littermates. Scale bars = 50 μm (left) and 20 μm (right). (**b**) Epidermal thickness was measured on 10 randomly chosen images from five to six mice of each genotype. (**c**) Immunofluorescence staining for KRT14 (green) and filaggrin (red) (**e**) p63 (left) or PCNA (right), in a PTH2 receptor knockout mouse or its littermate's epidermis. White bars = 20 μm. (**d**, **f**) Calculated immunofluorescence staining area of filaggrin and PCNA. Data are means ± SEM, n = 6. $^{**}P < 0.01$ $^{*}P < 0.05$. H&E, hematoxylin and eosin; KRT14, keratin-14; PCNA, proliferating cell nuclear antigen; PTH2R, PTH second receptor.